

## Article

# Study on Mechanisms for Improving Quality and Whiteness of Phosphogypsum Based on Process Mineralogy Analysis

Wanqiang Dong <sup>1</sup>, Ru'an Chi <sup>1,2,\*</sup>, Wanxin Guo <sup>1</sup>, Xiangyi Deng <sup>1</sup>, Zhuo Chen <sup>1</sup> and Haodong Chen <sup>3</sup>

<sup>1</sup> School of Resources and Safety Engineering, Wuhan Institute of Technology, Wuhan 430205, China; honestman08@163.com (W.D.); 13103568659@163.com (W.G.); xiangyideng@126.com (X.D.); 23051105@wit.edu.cn (Z.C.)

<sup>2</sup> Hubei Three Gorges Laboratory, Yichang 443007, China

<sup>3</sup> School of Chemistry and Environmental Engineering, Wuhan Institute of Technology, Wuhan 430205, China; vokeieschen@outlook.com

\* Correspondence: rac@wit.edu.cn; Tel.: +86-18-164-241-336

**Abstract:** Because of its low whiteness, complex composition, radioactivity and high impurity percentage, the usage of phosphogypsum (PG) resources is limited. A theoretical foundation for upgrading and bleaching PG can be obtained by researching the presence and status of impurities in the material and its symbiotic connection with gypsum. This paper makes use of an automatic mineral phase analyzer, optical microscope, XRF, XRD and SEM-EDS. After analyzing the chemical makeup of PG, phase composition and particle size composition, the distribution law and symbiotic interaction between impurities and gypsum in various particle sizes were discovered. Using a flotation test, the process mineralogy analysis results were confirmed. According to the XRF and XRD study results, the primary impurity elements in PG are Si, P and F. Si is more abundant in PG that is between +850  $\mu\text{m}$  and  $-37.5 \mu\text{m}$  in size. The concentrations of gypsum and quartz in PG are 82.59% and 8.73%, respectively, according to the results of XRD and process mineralogy. The monomer dissociation degree of the gypsum mineral phase is as high as 90.47%. Gibbsite and pyrite are the primary causes of the low whiteness of PG and are clearly related to the quartz mineral phase. The coupling process of “flotation + pickling” produced purified PG with a purity of 95.35%, whiteness of 70.76% and SiO<sub>2</sub> content of 2.73%. The quality met the first-class index standards of PG in GB/T23456-2018.

**Keywords:** phosphogypsum; process mineralogy; degree of dissociation; whiteness; flotation



**Citation:** Dong, W.; Chi, R.; Guo, W.; Deng, X.; Chen, Z.; Chen, H. Study on Mechanisms for Improving Quality and Whiteness of Phosphogypsum Based on Process Mineralogy Analysis. *Minerals* **2024**, *14*, 471. <https://doi.org/10.3390/min14050471>

Academic Editor: Mostafa Benzaazoua

Received: 13 March 2024

Revised: 11 April 2024

Accepted: 25 April 2024

Published: 29 April 2024



**Copyright:** © 2024 by the authors. Licensee MDPI, Basel, Switzerland. This article is an open access article distributed under the terms and conditions of the Creative Commons Attribution (CC BY) license (<https://creativecommons.org/licenses/by/4.0/>).

## 1. Introduction

Phosphogypsum (PG) is an industrial solid waste produced during the production of phosphoric acid through the wet process [1]. In 2021, the newly increased production of PG was estimated to be 80 million tons and the cumulative stacking capacity was up to 800 million tons [2]. The continuous dissolution of phosphorus and fluorine impurities in accumulated PG causes regional environmental pollution (including water and soil pollution) as well as a high-pressure ecological environment. Therefore, it is very critical to realize the harmlessness, recycling and reduction of PG [3–5]. Resource utilization is one of the key ways for effective PG utilization at present. However, due to the high impurity content, complex composition, radioactivity and low whiteness of PG, the utilization level of its comprehensive resources has been seriously restricted [6–10]. Therefore, exploring the occurrence regularity of the main color-causing minerals in PG and developing technology to enhance the quality and whiteness of PG is of great significance to realize its high-value comprehensive exploitation.

During the phosphoric acid production process (also known as the “wet process of phosphoric acid”), phosphate rock hydrolyzed with sulfuric acid forms a supersaturated solution of calcium sulfate in the acidolysis reaction tank and the CaSO<sub>4</sub>·2H<sub>2</sub>O crystal grows

rapidly in the supersaturated solution [11,12]. During crystal growth, large amounts of unreacted fluorapatite, quartz impurities, colloidal, soluble phosphorus and other impurities of phosphate rock composition also precipitate and get included in the produced PG. Hence, the production of PG can be considered a chemical mineralization process. Therefore, the quality and whiteness of PG can be improved by employing mineral processing methods. Currently, investigators have conducted research on PG purification through flotation and coupling-flotation processes [13–15]. Qi et al. [16] obtained gypsum concentrate with 69.2% whiteness and 97.24% purity through a reverse-positive flotation process. Wang et al. [17] increased the whiteness of PG from 31.3% to 58% through a closed-circuit flotation test. The purity of  $\text{CaSO}_4 \cdot 2\text{H}_2\text{O}$  obtained in the concentrate reached above 95% with a concentrate efficiency of 65%. The purity of  $\text{CaSO}_4 \cdot 2\text{H}_2\text{O}$  in PG can be improved via the flotation process, but the purification efficiency of PG flotation is low and a large amount of tailings produced during flotation causes secondary pollution. The main reason is that the mineral phase composition of PG impurity is complex and the occurrence regularity of various mineral phases is unclear. The investigation of the basic mineralogical data of the PG process helps to achieve the goal of full utilization of PG resources [18].

Process mineralogical characteristics mainly include the composition, content, dissociation degree and embedded characteristics of the mineral phase, which are capable of giving basic research parameters to realize the efficient exploitation of minerals [19–21]. The process of mineralogy parameters can be determined through microscopic investigations and by the automatic mineral analysis system [22–24]. Microscopic study is one of the crucial tools for processing mineralogical studies. Mineral composition, content, embedding relationships and particle size composition of raw ore or mineral processing products can be determined through observation and identification of optical microscopes such as binocular stereomicroscope, transmission polarizing microscope and reflection polarizing microscope [25–27]. Automatic mineral characterization system (AMCIS) is an effectual automated mineral analysis system based on high-resolution scanning electron microscopy (SEM) and energy dispersive spectroscopy (EDS). Such an effective system is able to realize the grainy treatment of backscattered electron images of samples, distinguish various mineral phases and automatically collect their energy spectrum data. It then accurately identify minerals by using X-rays generated from energy spectrum and establish the standard database of sample minerals and relevant factors, including mineral symbiosis, intergrowth and dissociation degree, after automatic fitting and calculation by computer [28–30].

A brief survey of the literature reveals that little research has been devoted to the process mineralogy of PG in the academic community [31,32]. This study intends to employ the research method of process mineralogy to explore the mineral phase composition, the dissociation degree of essential minerals and the occurrence characteristics of the color-causing mineral phase in PG. It is hoped that this exploration provides theoretical support for improving the quality and whiteness of PG in the flotation process.

## 2. Experimental Materials and Methods

### 2.1. Experimental Reagents and Raw Materials

Dodecylamine is the cationic collector used for flotation, and 98% concentrated sulfuric acid is diluted to create the acid wash solution.  $\text{HNO}_3$  and  $\text{NaOH}$  are examples of pH regulators, and deionized water is used in research. The China National Pharmaceutical Group provided the analytical quality dodecylamine,  $\text{H}_2\text{SO}_4$ ,  $\text{HNO}_3$  and  $\text{NaOH}$  used in the experiment. The PG samples used in the experiment came from one Yichang, China-based enterprise that produces phosphorus fertilizer.

### 2.2. Analysis and Testing Methods

A Bruker D8 Advance X-ray diffractometer (XRD) is used to examine the phase composition of the PG samples, while a RIGAKU ZSX Primus X-ray fluorescence spectrometer (XRF) is used to analyze the materials' chemical composition. AMICS is used to investigate

the mineral content, composition and embedding properties of PG samples. The powder samples of PG are dried to a consistent weight at 45 °C for AMICS analysis. After that, they are embedded in epoxy resin to create circular specimens that have a diameter of 30 mm. Once the specimens have been polished and coated in gold, they are put under an electron microscope. The samples' whiteness is measured by ZB-B whiteness meter. Several measurements are made in order to get the average result. The content of  $\text{CaSO}_4 \cdot 2\text{H}_2\text{O}$  is determined using the method specified in GB/T 2018-23456 PG [33].

### 2.3. Flotation Experiment Method

A dosage of 200 g/t of dodecylamine and a pH of 2.0 result in flotation for three minutes, which generates concentrate. Then, to obtain extensively purified PG samples, pickling treatment is carried out at a liquid–solid ratio of 5:1, pickling period of 2 h and temperature of 25 °C using 5%  $\text{H}_2\text{SO}_4$  solution as the leaching solution. Figure 1 illustrates the PG purification procedure utilizing the “flotation-acid leaching” combined process.

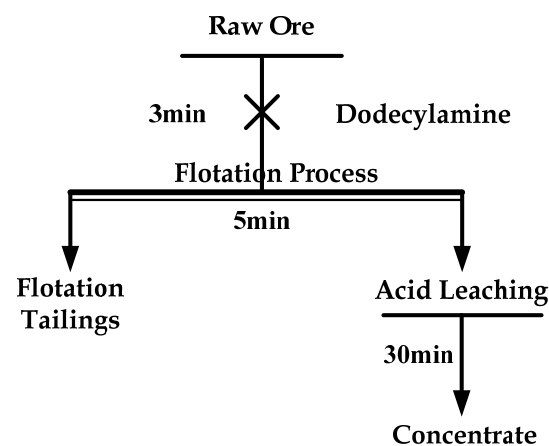


**Figure 1.** Process flowchart for direct flotation coupled with acid leaching.

## 3. Results

### 3.1. Analysis of Mineral Composition of PG

The PG samples used in this study are collected from the PG produced during the production of phosphoric acid through a wet process (the so-called “dihydrate process”) by a phosphate fertilizer manufacturing company in Yichang, Hubei Province of China. The collected samples are dried to a constant weight in a drying oven at 45 °C via a standard sampling method and then placed in a desiccator for storage. The composition of the mineral phase was analyzed and determined using XRD and the obtained results are presented in Figure 2.

The results of the XRD analysis reveal that the main mineral phases of PG are calcium sulfate dihydrate, quartz and incompletely reacted fluorapatite and the intensity at the diffraction peaks of the impurity mineral phase (such as fluorapatite) is weak. This is mainly attributed to the fact that the mineral impurity content is much lower than calcium sulfate dihydrate and quartz and its characteristic peak is masked by the strong absorption peak of calcium sulfate dihydrate and quartz. It should be emphasized that although XRD analysis is often not able to precisely identify minerals with low content, it may accurately identify the phase information of important minerals. Furthermore, as Yang et al. [34] have shown, important mineralogical details including the micro-morphology, particle size and mineral development relationships cannot be obtained by XRD analysis.

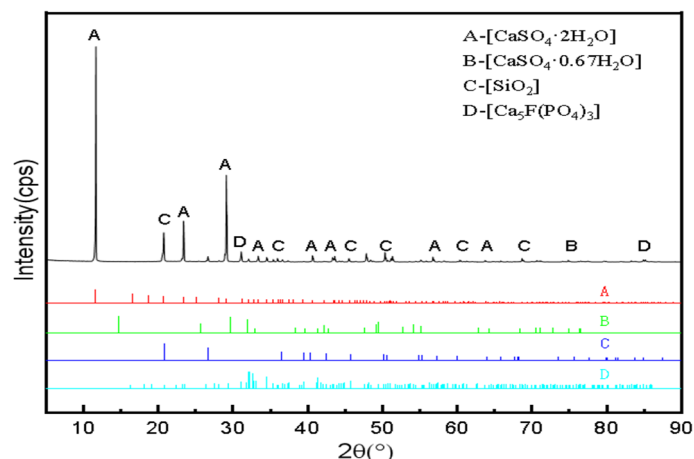


**Figure 2.** XRD analysis results of PG.

### 3.2. Chemical Composition and Particle Size Distribution of PG

The results of the XRF analysis are provided in Table 1. CaO, SO<sub>3</sub> and SiO<sub>2</sub> are the main chemical components of PG and their contents in order are 37.30, 51.83 and 7.66%. P<sub>2</sub>O<sub>5</sub> and Al<sub>2</sub>O<sub>3</sub> are secondary components, with contents of 1.28% and 0.39%, respectively. In addition, they also contain a small amount of K<sub>2</sub>O, Fe<sub>2</sub>O<sub>3</sub>, MgO and TiO<sub>2</sub>, the content of which is less than 0.2%. The results of the chemical composition analysis indicate that the main component of PG is calcium sulfate, whereas phosphorus and fluorine represent the main impurity elements. The presence of fluorine was depicted from XRD pattern, since XRF method does not identify this element.

**Table 1.** Chemical composition and content of PG.

Element	SO <sub>3</sub>	CaO	SiO <sub>2</sub>	P <sub>2</sub> O <sub>5</sub>	K <sub>2</sub> O	Al <sub>2</sub> O <sub>3</sub>	Na <sub>2</sub> O
Content%	51.83	37.30	7.66	1.28	0.53	0.39	0.19
Element	Fe <sub>2</sub> O <sub>3</sub>	TiO <sub>2</sub>	MnO	MgO	NiO	SrO	BaO
Content%	0.42	0.14	0.008	0.059	0.0034	0.071	0.12

The formation process of PG in the wet process phosphoric acid reaction system can be considered as a chemical ore-forming process. In this process, with the irregular growth of calcium sulfate dihydrate crystal, impurity mineral phases in PG particles with various particle sizes show different occurrence characteristics. To discover the enrichment law of phosphorus, fluorine, iron, aluminum and other impurity elements in PG with different particle sizes, we investigate the embedded characteristics of PG elements with various particle sizes. The results showed that phosphorus could be enriched in PG particles with particle size > 0.150 mm and particle size < 0.0374 mm, which presents the rule of “enrichment at both ends”. The analysis results of the chemical composition of PG in different particle sizes are provided in Table 2.

Based on the analysis results of chemical elements in PG with various particle sizes, Pearson’s correlation coefficient could be used to analyze the correlation between chemical elements in PG and investigate the effect of PG particle size on the occurrence of chemical elements. The results of the analysis are presented in Figure 3.

The results of the correlation analysis showed that there would exist a strong negative correlation between the CaSO<sub>4</sub> content and the particle size, which showed that with the increase in the size of the PG particles, the CaSO<sub>4</sub> content demonstrated a downward trend and the minimum calcium sulfate dihydrate content appeared in the 400-mesh particle size. The results indicated that there was a negative correlation between SiO<sub>2</sub> and particle size, indicating that the content of SiO<sub>2</sub> decreases with increasing particle size of PG. The correlation coefficient between Al<sub>2</sub>O<sub>3</sub> and particle size was between −0.0708 and −0.0518, demonstrating a weak negative correlation, indicating that Al<sub>2</sub>O<sub>3</sub> content reduces with

increasing particle size. The correlation coefficient between the P<sub>2</sub>O<sub>5</sub> content and the particle size was between −0.1399 and 0.2633. As shown in Figure 3a, when the particle size of PG is less than 150 μm, there is an increasing trend in P<sub>2</sub>O<sub>5</sub> content with increasing particle size. The obtained results revealed that soluble phosphorus and fluorine were the main impurity elements of PG. A strong correlation between the crystal grain size and the soluble phosphorus content was detected in the wet process phosphoric acid reaction system as well as in the calcium sulfate acid system. Figure 3b presents the correlation analysis results among elements in PG. It is worth mentioning that iron and aluminum exhibit a strong positive correlation with silicon and a strong negative correlation with calcium. Relevant studies reveal that iron mineral phases in PG are mainly pyrite and limonite and aluminum minerals are mainly feldspar, gibbsite and chlorite. The iron and aluminum mineral phases in PG may essentially coexist with quartz minerals.

**Table 2.** Chemical composition of PG with various particle sizes.

Element \ Particle Size/μm	<37.4	37.4–75	75–105	105–150	150–250	250–830
Na <sub>2</sub> O	0.18	0.15	0.15	0.19	0.23	0.19
MgO	0.076	0.047	0.05	0.059	0.069	0.062
Al <sub>2</sub> O <sub>3</sub>	0.43	0.35	0.35	0.39	0.44	0.44
SiO <sub>2</sub>	12.92	7.69	7.60	7.66	8.78	8.64
P <sub>2</sub> O <sub>5</sub>	1.61	1.28	1.20	1.28	1.37	1.45
SO <sub>3</sub>	49.77	52.07	51.88	51.83	51.18	51.35
K <sub>2</sub> O	0.34	0.44	0.62	0.53	0.58	0.51
CaO	33.36	37.16	37.41	37.30	36.49	36.52
TiO <sub>2</sub>	0.19	0.14	0.13	0.14	0.17	0.13
MnO	0.007	-	-	0.008	-	0.008
Fe <sub>2</sub> O <sub>3</sub>	0.76	0.45	0.40	0.42	0.48	0.49
SrO	0.068	0.078	0.074	0.07	0.069	0.073
Y <sub>2</sub> O <sub>3</sub>	-	0.004	0.002	-	0.003	0.003
NiO	0.004	-	0.003	-	0.004	-
BaO	0.27	0.15	0.14	0.12	0.15	0.12

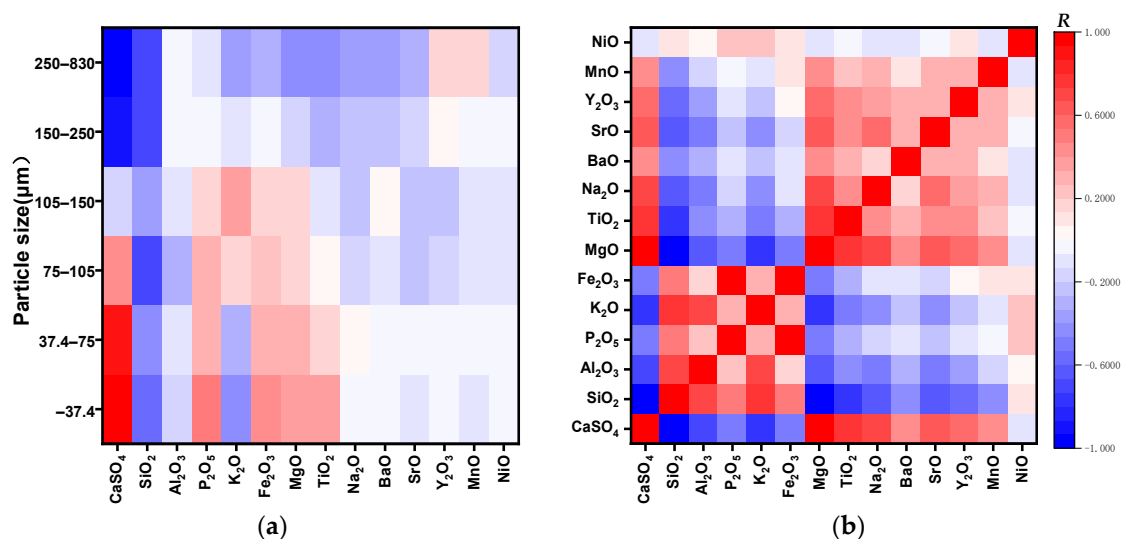


**Figure 3.** Heatmap used for analysis of correlation between (a) particle size and (b) chemical composition.

### 3.3. Embedded Characteristics of Essential Minerals in PG

#### 3.3.1. Optical Microscope Analysis

Mineral phase analysis is usually performed through microscopic observation and XRD analysis. Herein, the mineral phase of PG is qualitatively analyzed with a polarized microscope. The analysis results are presented in Figure 4.

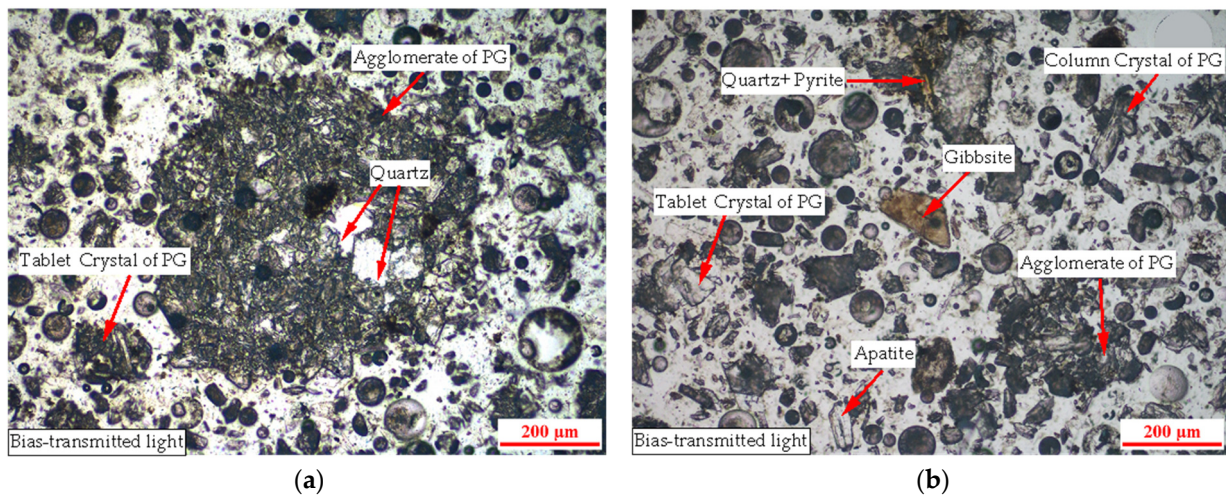


**Figure 4.** (a,b) Results of same PG sample from different locations via polarizing microscope.

The analysis results by optical microscope showed that the mineral phases in PG are gypsum, quartz, apatite and gibbsite. Under the optical microscope, gypsum (Gp) in the form of fine scales or fibrous grains or rhombic particles, colorless and transparent, slightly negative low protrusion, first-order gray-white interference color, with a group of intact cleavage visible parallel extinction, scattered and evenly distributed or aggregated in a mass distribution. Quartz (Qtz) is irregular and fragmented, colorless and transparent, first-order gray-white to first-order yellow-white, cracks in grains, sporadic distribution and pyrite can be seen in individual fragments; Apatite (Ap) is a short columnar or residual shape with high protrusion, first-order gray interference color, parallel extinction, sporadic distribution and particle size of 0.03–0.10 mm; Gibbsite (Gbs) is fragmented or fine aggregate, light brown, secondary interference color, sporadic distribution and particle size of 0.01–0.12 mm. The results of the microscopic analysis are able to qualitatively analyze the primary impurity mineral phases in PG, but the occurrence state of phosphorus, fluorine, potassium and other impure elements cannot be determined. Therefore, AMCIS is proposed for further analysis of the occurrence state of impurity elements in PG.

#### 3.3.2. Analysis of Automatic Mineral Analyzer

The automatic mineral analysis system is able to realize the quantitative analysis of the mineral phase composition in the target mineral. In the current investigations, the AMCIS automatic mineral analyzer is employed to examine the mineral phase composition and content in PG. The schematic representation of the analysis process is provided in Figure 5.

The mineral composition of the PG sample determined by the AMCIS automatic mineral analyzer is presented in Table 3. The test results reveal that the main mineral phases in PG are gypsum and quartz, which constitute 82.58% and 8.73%, respectively. The gypsum content is slightly lower than the 85% limit for first-grade PG specified in GB/T 2018-23456 PG. Potassium silicate and calcium aluminate represent the impurity mineral phases in PG whose content ranks second after quartz, and the mass ratio of potassium silicate mineral is 1.64%. The analysis results of the content of the main mineral phase based on the AMCIS automatic mineral analyzer indicate that if there is a need to improve the purity of PG products, the removal of quartz and potassium silicate impurity minerals in PG should be considered first.

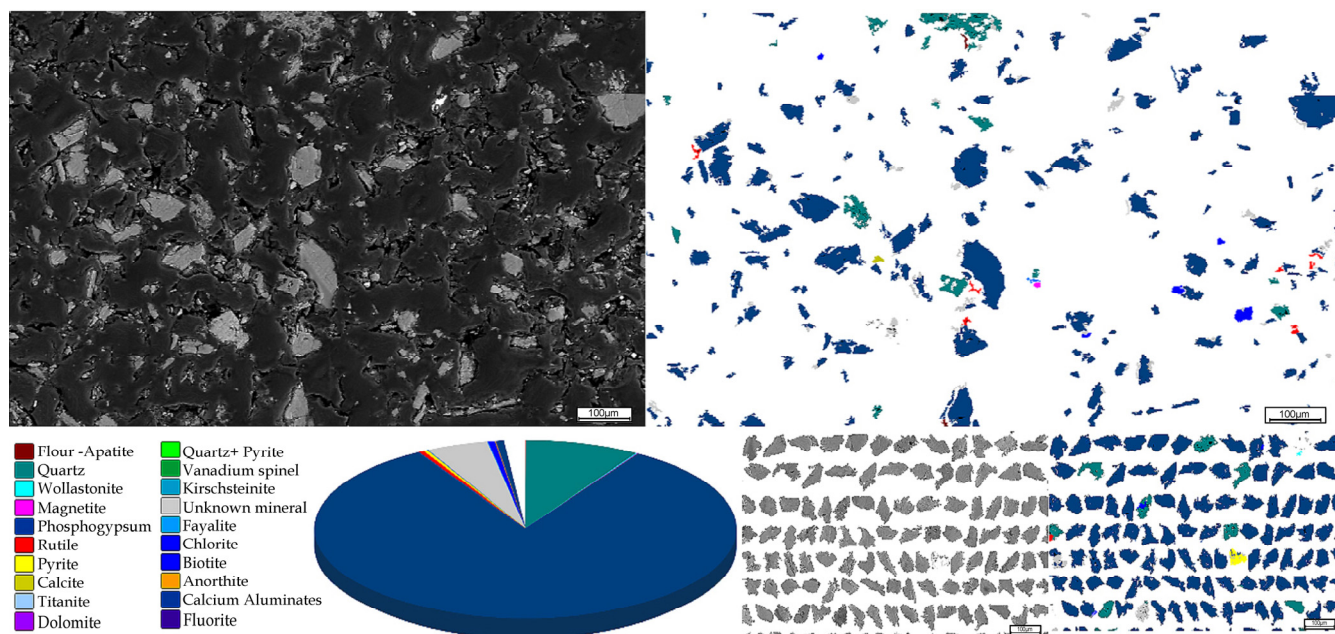


Figure 5. Determination of PG using AMCIS automatic mineral analyzer.

Table 3. Main mineral composition of PG.

Mineral	Weight Percentage (%)	Area Percentage (%)	Area (µm <sup>2</sup> )	Segment Number	Relative Error (%)
Gypsum	82.58	79.87	2,724,381	10,558	0.02
Quartz	8.73	8.45	288,266.8	1215	0.06
Potassium Silicate	1.64	1.59	54,145.04	236	0.13
Calcium Aluminates	0.62	0.6	20,375.62	184	0.15
Rutile	0.41	0.39	13,410.66	127	0.18
Biotite	0.3	0.23	7874.27	50	0.28
Pyrite	0.25	0.24	8288.05	41	0.31
Chlorite	0.21	0.22	7638.36	48	0.29
Wollastonite	0.13	0.12	4131.54	33	0.35
Anorthite	0.08	0.07	2348.49	18	0.47
Fayalite	0.07	0.06	2089.49	19	0.46
Flour-Apatite	0.06	0.06	2045.8	18	0.47
Calcite	0.05	0.05	1797.41	16	0.5
Magnetite	0.05	0.04	1390.49	13	0.55
Kirschsteinite	0.05	0.05	1612.05	11	0.6
Quartz + Pyrite	0.02	0.02	685.26	6	0.82
Titanite	0.02	0.01	496.78	4	1

The morphology and embedded characteristics of the main mineral particles of PG are illustrated in Figure 6. The embedded characteristics of gypsum, quartz and other minerals are also presented in Tables 4 and 5.

Table 4. Embedded characteristics of gypsum and other gangue minerals (%).

Mineral	Apatite	Quartz	Wollastonite	Rutile	Calcite	Titanite	Fayalite	Chlorite	Biotite	Other Minerals
Monomer dissociation						90.47				
Dyadic symbiosis	1.06	5.21	1.02	0.05	0.05	0.00	0.02	0.07	0.15	0.15
Three-membered encapsulation	0.00	0.02	0.00	0.00	0.00	0.01	0.00	0.00	0.01	0.07

**Table 5.** Embedded characteristics of single quartz mineral and other minerals (%).

Mineral	Wollastonite	PG	Rutile	Pyrite	Chlorite	Biotite
Monomer dissociation				84.80		
Dyadic symbiosis	1.00	11.34	0.70	0.44	0.60	0.00
Three-membered encapsulation	0.02	0.03	0.00	0.39	0.00	0.06

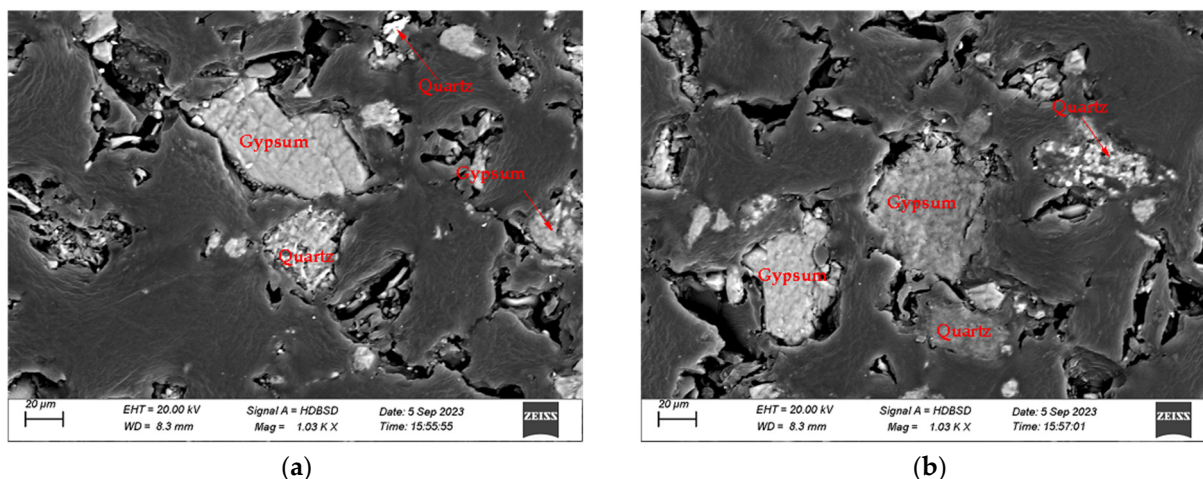
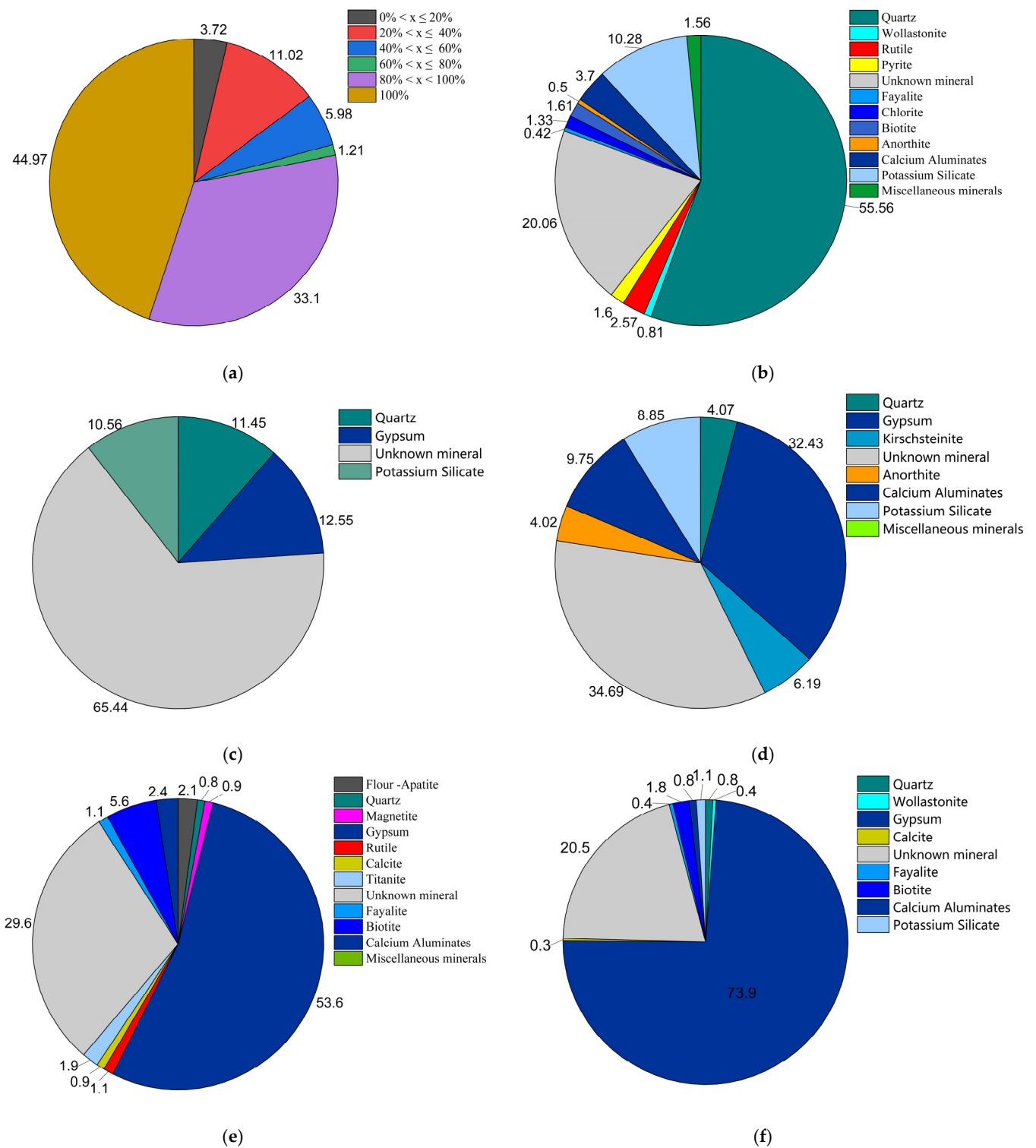
**Figure 6.** Morphology and embedded characteristics of main mineral particles of quartz and PG. (a) conjunctive edge relation (b) assorted relation.

Figure 6a presents the symbiosis of gypsum and quartz and Figure 6b illustrated the common junction structure of gypsum and quartz particles. The analysis results in Table 4 show that gypsum minerals in PG mainly exist in the form of monomer dissociation and the degree of monomer dissociation is 90.47%. The essential minerals with a binary symbiotic relationship with gypsum are quartz and fluorapatite, which are 5.21 and 1.06%, respectively. The ratio of minerals with a ternary symbiotic relationship with gypsum is relatively low and its cumulative ratio is less than 0.1%. The analysis results in Table 5 reveal that quartz mineral exists in PG in the form of monomer dissociation, and its monomer dissociation degree is 84.80%, which is slightly lower than the gypsum mineral phase. The essential minerals with a binary symbiotic relationship with quartz are PG, wollastonite and rutile, which in order account for 11.34%, 1.00% and 0.70%. Pyrite and quartz are mainly in ternary form, accounting for 0.39%. This analysis result is consistent with the strong correlation analysis results of Si and Fe elements in the high-correlation analysis that is shown in Figure 3b. Automated mineralogical analysis of AMCIS showed more order of occurrence of  $\text{SiO}_2$  and  $\text{Fe}_2\text{O}_3$  impurities in PG. The analysis results indicated that the separation of  $\text{SiO}_2$  in PG could effectively improve the content of gypsum components in PG. Additionally, it could achieve the collaborative removal of iron-containing mineral phase components and improve the whiteness of PG.

### 3.3.3. Occurrence Characteristics of Essential Impurity Minerals in Phosphogypsums

Based on the clarity of the mineral phase composition of PG in the sample, this paper examines the occurrence characteristics of impurity minerals such as quartz, rutile, biotite and chlorite in the essential mineral (gypsum) of principal PG. The analysis results are presented in Figure 7.



**Figure 7.** (a) Mass distribution ratio of mineral particles with various gypsum contents, and quantity ratio of each mineral content in the conjoined mineral with (b) 0%, (c) 0%–20%, (d) 20%–40%, (e) 40%–60% and (f) 60%–80% gypsum contents.

The mass distribution of particles with various gypsum contents is illustrated in Figure 7a. The gypsum content in PG particles is generally high, and the ratio of particles with 80%–100% gypsum content reaches 78.07%, whereas the mass ratio of gypsum minerals in the form of completely separated monomer minerals is 44.97%. Further, the particles containing 20%–40% gypsum contain 11.02% and the amount of gypsum in other particles

is less than 6%. It can be seen from Figure 7b that the mass ratio of quartz minerals in solid impurities of PG is 55.56%. For potassium silicate and unknown minerals in solid impurities, the corresponding mass ratio is 10.28% and 20.05%, respectively. It can be seen from Figure 7c that the mass ratios of quartz minerals, potassium silicate minerals and unknown minerals in order are 11.45%, 10.56% and 65.43% in interconnected minerals with 0%–20% content. Figure 7d displays that the mass ratio of quartz minerals with a gypsum content of 20%–40% is substantially lower than that of gypsum of 0%–20%, which is only 4.07%, 34.65% in unknown minerals and 8.85% in potassium silicate minerals. Figure 7e also demonstrates that the mass ratio of quartz in the conjoined mineral with 40%–60% gypsum content is only 0.82%, the unknown mineral is 29.60% and that of the biotite mineral is 5.63%. Figure 7f illustrates that the mass ratio of quartz mineral in the conjoined mineral with 60%–80% gypsum content is 0.81%, which is similar to that in the conjoined mineral with 60%–40% gypsum content. The mass ratio of unknown minerals is 20.48% and biotite minerals is 1.84%.

The distribution proportion analysis of gypsum minerals with various contents reveals that quartz is the primary impurity mineral of PG minerals. The symbiotic relationship between quartz and PG is significant in the conjoined mineral with less than 40% gypsum content, and the symbiotic phenomenon between unknown minerals and PG particles with low content is more significant. This part of the unknown mineral may represent an organic substance wrapped in PG, so the automatic mineral analysis system is not able to accurately match the mineral phases. According to the mass distribution law of gypsum minerals in various contents, PG particles essentially consist of gypsum minerals and the impurity mineral phase primarily occurs in particles with low gypsum content.

#### 3.4. Experiment on Improving Quality and Whiteness of PG by Flotation

The impurity gangue mineral phase in PG is mainly distributed in the gypsum mineral phase, and the gangue mineral phases such as pyrite and magnetite are mainly symbiotic with the quartz mineral phase. In addition, the impurity gangue mineral phases such as fluorapatite, rutile, biotite and chlorite are mainly symbiotic with the gypsum mineral phase. The dissociation degree of gypsum mineral phase monomer in PG is as high as 90.47%. Through flotation, the separation of gypsum and impurity mineral phases could be effectively performed, and then the whiteness and purity of PG can be improved. Based on process mineralogical analysis, the direct flotation approach coupled with acid pickling was employed to treat PG. As a result, the whiteness of purified PG reached 70.76%, the content of calcium sulfate dihydrate climbed up to 95.35% and the contents of soluble phosphorus and fluorine decreased to 0.098% and 0.052%, respectively.

FT-IR analysis was performed on the original sample of PG after quality and whiteness improvement using manual flotation with acid pickling. As demonstrated in Figure 8, the intensity of the distinctive O-S-O absorption peaks at  $596\text{ cm}^{-1}$  and  $671\text{ cm}^{-1}$  is higher in the “positive flotation + acid washing” coupling procedure for treating PG than in the original PG sample. This improvement might result from  $\text{CaSO}_4 \cdot 2\text{H}_2\text{O}$  being the primary ingredient in the test sample [35,36]. Following the coupling process treatment, the concentration of  $\text{CaSO}_4 \cdot 2\text{H}_2\text{O}$  rises considerably, which significantly enhances the distinctive O-S-O absorption peaks in the  $400\text{--}700\text{ cm}^{-1}$  range. Furthermore, at  $1142\text{ cm}^{-1}$ , a notable enhancement in the intensity of the distinctive absorption peak of the anti-symmetric stretching vibration of  $\text{SO}_4$  is detected in the  $\text{CaSO}_4 \cdot 2\text{H}_2\text{O}$  crystal molecule [37].

SEM-EDS mapping analysis was performed on the original PG, and the quality and whiteness of the sample were both improved by direct flotation with acid pickling. Figure 9 and Table 6 present the SEM images and the chemical composition of the mineral phase in PG. The mass ratio of calcium in purified PG was remarkably increased from 33.40% in raw ore to 58.54%, and the contents of Si and Fe showed a decreasing trend from 12.91% and 0.76% in raw ore to 0.11% and 0.51%, respectively. In tailings, calcium content decreased to 1.81% and Si increased to 78.06%, indicating a clear enrichment. The mass ratio of Fe was obtained as 13.63%, which was not as enriched as Si, indicating that Fe impurities

were partially dissolved and transferred to the pickling solution during pickling. SEM mapping analysis revealed that the direct flotation process combined with acid pickling could achieve the collaborative separation of Si and Fe impurities in PG samples. Lehr et al. found a high correlation between the presence of iron impurities and silicon elements in phosphogypsum [38]. The mapping analysis results of PG samples obtained by the combined process in this study are highly consistent with the research conclusions of Lehr et al.

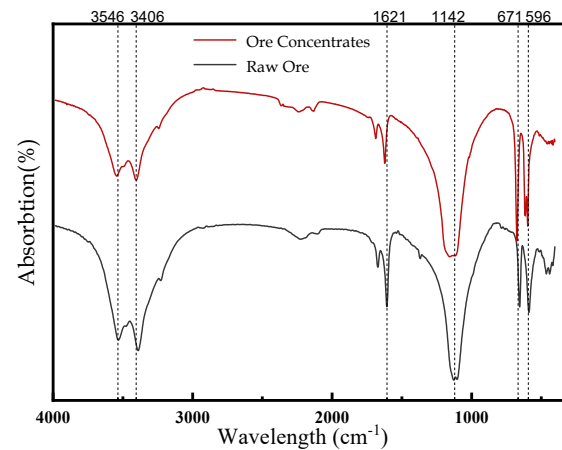


**Figure 8.** FI-TR analysis and test results of original PG sample and improved PG concerning quality and whiteness.

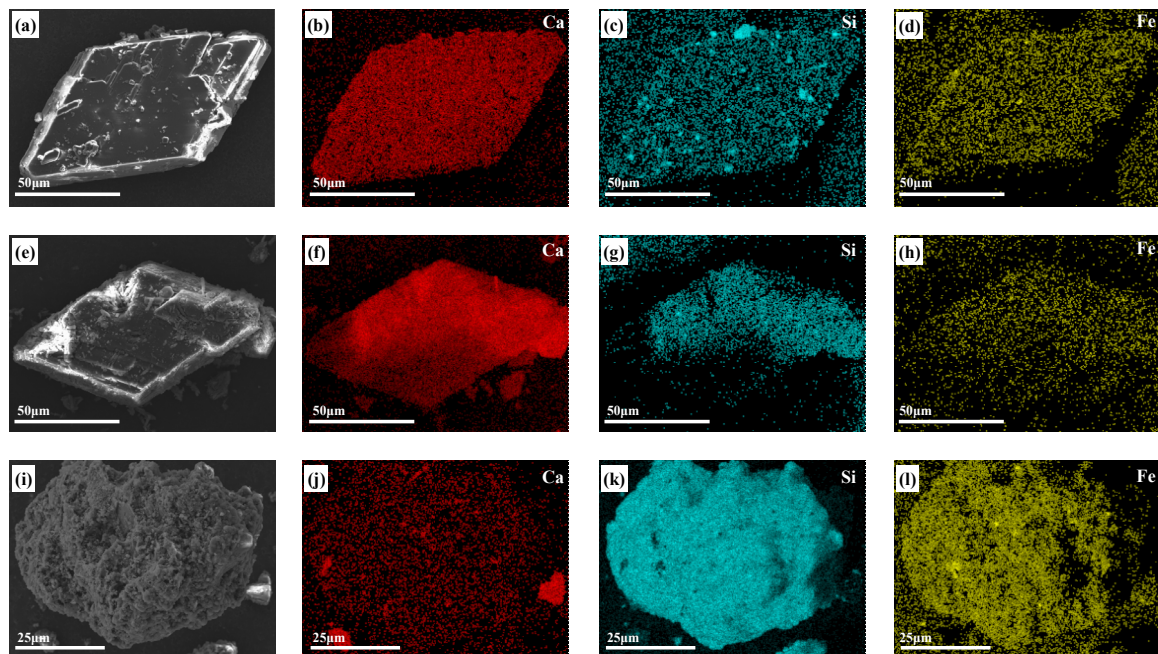


**Figure 9.** SEM-EDS mapping analysis results of original PG sample, flotation concentrate, and tailings: (a,e,i) SEM images of test samples, (b,f,j) mapping analysis results of Ca element in test samples, (c,g,k) mapping analysis results of Si element in test samples, (d,h,l) mapping analysis results of Fe element in test samples.

**Table 6.** SEM-EDS mapping analysis of element composition in samples.

Mineral	Element (wt.%)							
	Ca	S	Si	P	F	Fe	Al	K
Raw ore	33.40	49.82	12.91	1.61	0.35	0.76	0.43	0.34
Ore concentrates	58.54	38.98	0.11	1.83	0.00	0.51	0.00	0.03
Mine tailing	1.81	4.29	78.06	2.15	0.00	13.63	0.01	0.05

#### 4. Conclusions

- (1) The analysis of mineral phases demonstrated that the main phases in PG include calcium sulfate dihydrate, quartz and incompletely reacted fluorapatite. The results of the chemical composition analysis revealed that the main component of PG was calcium sulfate, whereas phosphorus and fluorine were the main impurity elements and quartz showed an obvious enrichment phenomenon in fine-grained PG particles.
- (2) The process mineralogical analysis approach showed that gangue minerals with a binary symbiotic relationship in PG include fluorapatite, quartz, wollastonite, rutile, calcite, biotite, calcium aluminate and chlorite. Among them, the gangue mineral and fluorapatite mineral phases represent the main symbiotic impurity minerals. The dissociation degree of the gypsum mineral phase in PG is as high as 90.47% and the impurity mineral phase is majorly enriched in the conjoined mineral with 20%–60% gypsum. Through the coupling process of “flotation + pickling,” the purity of  $\text{CaSO}_4 \cdot 2\text{H}_2\text{O}$  could reach 95.35%, the whiteness could touch 70.76% and the contents of soluble phosphorus and fluorine could reach 0.098% and 0.052%, respectively.
- (3) The production process of PG can be considered a chemical mineralization process. The process mineralogical analysis approach can be employed to quantitatively analyze the composition and content of impurity mineral phases and the dissociation degree of main mineral phases in PG, which can provide a new way for PG impurity phase analysis and a theoretical basis for PG deep purification and resource utilization.

**Author Contributions:** Methodology, R.C.; software, H.C. and W.G.; writing—original draft, W.D.; writing—review and editing, W.D. and Z.C.; supervision, X.D. and Z.C.; project administration, Z.C.; funding acquisition, R.C. and W.D. All authors have read and agreed to the published version of the manuscript.

**Funding:** This work financially supported by the National Key Research and Development Program Foundation of China (No. 2022YFC3902702), the Chief Scientist Project Foundation of Three Gorges Laboratory (No. SXCS2204) and Hubei Three Gorges Laboratory Open Fund Project (No. SK211002).

**Data Availability Statement:** The original contributions presented in the study are included in the article.

**Conflicts of Interest:** The authors declare no conflicts of interest.

#### References

1. Wang, B.; Yang, L.; Luo, T.; Cao, J. Study on the kinetics of hydration transformation from hemihydrate phosphogypsum to dihydrate phosphogypsum in simulated wet process phosphoric acid. *ACS Omega* **2021**, *6*, 7342–7350. [[CrossRef](#)]
2. Cui, R. Status of comprehensive utilization of phosphogypsum in China in 2021 and suggestions. *Phosphate Compd. Fertil.* **2022**, *37*, 3.
3. Cao, J.; Wang, Z.; Ma, X.; Yang, X.; Zhang, X.; Pan, H.; Wu, J.; Xu, M.; Lin, L.; Zhang, Y. Promoting coordinative development of phosphogypsum resources reuse through a novel integrated approach: A case study from China. *J. Clean. Prod.* **2022**, *374*, 134078. [[CrossRef](#)]
4. Chernysh, Y.; Yakhnenko, O.; Chubur, V.; Roubík, H. Phosphogypsum recycling: A review of environmental issues, current trends, and prospects. *Appl. Sci.* **2021**, *11*, 1575. [[CrossRef](#)]
5. Silva, L.F.; Oliveira, M.L.; Crissien, T.J.; Santosh, M.; Bolivar, J.; Shao, L.; Dotto, G.L.; Gasparotto, J.; Schindler, M. A review on the environmental impact of phosphogypsum and potential health impacts through the release of nanoparticles. *Chemosphere* **2022**, *286*, 131513. [[CrossRef](#)]

6. Wu, F.; Ren, Y.; Qu, G.; Liu, S.; Chen, B.; Liu, X.; Zhao, C.; Li, J. Utilization path of bulk industrial solid waste: A review on the multi-directional resource utilization path of phosphogypsum. *J. Environ. Manag.* **2022**, *313*, 114957. [[CrossRef](#)]
7. Qin, X.; Cao, Y.; Guan, H.; Hu, Q.; Liu, Z.; Xu, J.; Hu, B.; Zhang, Z.; Luo, R. Resource utilization and development of phosphogypsum-based materials in civil engineering. *J. Clean. Prod.* **2023**, *387*, 135858. [[CrossRef](#)]
8. Murali, G.; Azab, M. Recent research in utilization of phosphogypsum as building materials. *J. Mater. Res. Technol.* **2023**, *25*, 960–987. [[CrossRef](#)]
9. Yang, J.; Liu, S.; Wang, Y.; Huang, Y.; Yuxin, S.; Dai, Q.; Liu, H.; Ma, L. Phosphogypsum resource utilization based on thermodynamic analysis. *Chem. Eng. Technol.* **2022**, *45*, 776–790. [[CrossRef](#)]
10. Ennaciri, Y.; Bettach, M. The chemical behavior of the different impurities present in Phosphogypsum: A review. *Phosphorus Sulfur Silicon Relat. Elem.* **2024**, *199*, 129–148. [[CrossRef](#)]
11. Fang, K.; Xu, L.; Yang, M.; Chen, Q. One-step wet-process phosphoric acid by-product CaSO<sub>4</sub> and its purification. *Sep. Purif. Technol.* **2023**, *309*, 123048. [[CrossRef](#)]
12. Wang, B.; Yang, L.; Cao, J. The influence of impurities on the dehydration and conversion process of calcium sulfate dihydrate to  $\alpha$ -calcium sulfate hemihydrate in the two-step wet-process phosphoric acid production. *ACS Sustain. Chem. Eng.* **2021**, *9*, 14365–14374. [[CrossRef](#)]
13. Fang, J.; Ge, Y.; Chen, Z.; Xing, B.; Bao, S.; Yong, Q.; Chi, R.; Yang, S.; Ni, B.-J. Flotation purification of waste high-silica phosphogypsum. *J. Environ. Manag.* **2022**, *320*, 115824. [[CrossRef](#)]
14. Li, J.; Guo, Y.; Fan, P.; Li, H.; Chen, C.; Xu, S.; Du, L. A flotation combined extraction process for improving the whiteness of phosphogypsum. *Physicochem. Probl. Miner. Process.* **2023**, *59*, 170043. [[CrossRef](#)]
15. Qing, J.; Zhao, D.; Zeng, L.; Zhang, G.; Zhou, L.; Du, J.; Li, Q.; Cao, Z.; Wu, S. Comprehensive recovery of rare earth elements and gypsum from phosphogypsum: A wastewater free process combining gravity separation and hydrometallurgy. *J. Rare Earths* **2024**. [[CrossRef](#)]
16. Qi, M.; Peng, W.; Wang, W.; Cao, Y.; Fan, G.; Huang, Y. Simple and efficient method for purification and recovery of gypsum from phosphogypsum: Reverse-direct flotation and mechanism. *J. Mol. Liq.* **2023**, *371*, 121111. [[CrossRef](#)]
17. Wang, H.; You, X.; Tian, J.; Cheng, X.; Wang, J. Study on Pretreatment of Phosphogypsum and Preparation of Non Burning Building Materials. *IOP Conf. Ser. Earth Environ. Sci.* **2021**, *668*, 012076. [[CrossRef](#)]
18. Ma, L.; Zhang, H.; Wang, X.; Chen, L. Application and Development Prospects of Phosphogypsum in Different Phases: A Review. *Preprints* **2023**. [[CrossRef](#)]
19. Li, H.; Han, Y.; Jin, J.; Gao, P.; Zhou, Z. Process mineralogy approach to optimize curing-leaching in vanadium-bearing stone coal processing plants. *Int. J. Min. Sci. Technol.* **2023**, *33*, 123–131. [[CrossRef](#)]
20. Yarıluğkal Altınışık, C.; Cebeci, Y.; Sis, H.; Kalender, L. A Process Mineralogy Approach to the Flotation of Complex Lead–Zinc Ores from Görgü (Malatya) Region. *Min. Metall. Explor.* **2022**, *39*, 1219–1232. [[CrossRef](#)]
21. Schulz, B.; Sandmann, D.; Gilbricht, S. SEM-based automated mineralogy and its application in geo-and material sciences. *Minerals* **2020**, *10*, 1004. [[CrossRef](#)]
22. Tuhý, M.; Hrstka, T.; Ettler, V. Automated mineralogy for quantification and partitioning of metal (loid) s in particulates from mining/smelting-polluted soils. *Environ. Pollut.* **2020**, *266*, 115118. [[CrossRef](#)]
23. Donskoi, E.; Manuel, J.; Hapugoda, S.; Poliakov, A.; Raynlyn, T.; Austin, P.; Peterson, M. Automated optical image analysis of goethitic iron ores. *Miner. Process. Extr. Metall.* **2022**, *131*, 14–24. [[CrossRef](#)]
24. Liu, H.; Ren, Y.-L.; Li, X.; Hu, Y.-X.; Wu, J.-P.; Li, B.; Luo, L.; Tao, Z.; Liu, X.; Liang, J. Rock thin-section analysis and identification based on artificial intelligent technique. *Pet. Sci.* **2022**, *19*, 1605–1621. [[CrossRef](#)]
25. Cardoso-Fernandes, J.; Silva, J.; Perrotta, M.M.; Lima, A.; Teodoro, A.C.; Ribeiro, M.A.; Dias, F.; Barrès, O.; Cauzid, J.; Roda-Robles, E. Interpretation of the reflectance spectra of lithium (Li) minerals and pegmatites: A case study for mineralogical and lithological identification in the Fregeneda-Almendrea Area. *Remote Sens.* **2021**, *13*, 3688. [[CrossRef](#)]
26. Donskoi, E.; Poliakov, A. Advances in optical image analysis textural segmentation in ironmaking. *Appl. Sci.* **2020**, *10*, 6242. [[CrossRef](#)]
27. Okada, N.; Maekawa, Y.; Owada, N.; Haga, K.; Shibayama, A.; Kawamura, Y. Automated identification of mineral types and grain size using hyperspectral imaging and deep learning for mineral processing. *Minerals* **2020**, *10*, 809. [[CrossRef](#)]
28. Pszonka, J.; Schulz, B.; Sala, D. Application of mineral liberation analysis (MLA) for investigations of grain size distribution in submarine density flow deposits. *Mar. Pet. Geol.* **2021**, *129*, 105109. [[CrossRef](#)]
29. Yang, J.; Zhu, P.; Ma, S. Application of MLA in analysis of limonite bearing-zinc ore. *J. Phys. Conf. Ser.* **2021**, *2044*, 012097. [[CrossRef](#)]
30. Rodrigues, R.d.S.; Brandao, P.R.G. MLA and optical microscopy as complementary techniques to the iron ore geometallurgical studies. *REM-Int. Eng. J.* **2021**, *75*, 45–54. [[CrossRef](#)]
31. Fornes, I.V.; Vaičiukynienė, D.; Nizevičienė, D.; Doroševs, V.; Michalik, B. A comparative assessment of the suitability of phosphogypsum from different origins to be utilised as the binding material of construction products. *J. Build. Eng.* **2021**, *44*, 102995. [[CrossRef](#)]
32. Xiao, J.; Lu, T.; Zhuang, Y.; Jin, H. A novel process to recover gypsum from phosphogypsum. *Materials* **2022**, *15*, 1944. [[CrossRef](#)]
33. GB/T 23456-2018; Phosphogypsum. China Federation of Building Materials: Beijing, China, 2018.

34. Bo, Y.; Li, Y.; Wenxiang, M.; Maosen, S.; Tao, L.; Hongdong, Y. Application of X-ray Powder Diffraction Analysis in Bayan Obo Deposit with Microprobe Slice. *Nonferrous Met.* **2021**, *6*, 34–42.
35. Zhang, H.; Chai, W.; Cao, Y. Flotation separation of quartz from gypsum using benzyl quaternary ammonium salt as collector. *Appl. Surf. Sci.* **2022**, *576*, 151834. [[CrossRef](#)]
36. Nakamoto, K. Infrared and Raman Spectra of Inorganic and Coordination Compounds. *Am. Cancer Soc.* **2006**, *51*, 154.
37. Qiao, X. *Flotation Performance and Mechanism of Reagents Based on Dodecylamine and 2-Octanol*; Taiyuan University of Technology: Taiyuan, China, 2020.
38. Lehr, J.; Frazier, A.W.; Smith, J. Phosphoric acid impurities, precipitated impurities in wet-process phosphoric acid. *J. Agric. Food Chem.* **1966**, *14*, 27–33. [[CrossRef](#)]

**Disclaimer/Publisher’s Note:** The statements, opinions and data contained in all publications are solely those of the individual author(s) and contributor(s) and not of MDPI and/or the editor(s). MDPI and/or the editor(s) disclaim responsibility for any injury to people or property resulting from any ideas, methods, instructions or products referred to in the content.